Fibrogenic fibroblasts increase intercellular adhesion strength by reinforcing individual OB-cadherin bonds

Philippe Pittet[1], Kyumin Lee[2], Andrzej J. Kulik[2], Jean-Jacques Meister[1] and Boris Hinz[1,*]

[1]Laboratory of Cell Biophysics, [2]Laboratory of Nanostructures and Novel Electronic Materials, Institute of Physics of the Complex Matter, Ecole Polytechnique Fédérale de Lausanne (EPFL), CH-1015 Lausanne, Switzerland

*Author for correspondence (e-mail: boris.hinz@epfl.ch)

Accepted 31 December 2007
Journal of Cell Science 121, 877-886 Published by The Company of Biologists 2008
doi:10.1242/jcs.024877

Summary

We have previously shown that the switch from N-cadherin to OB-cadherin expression increases intercellular adhesion between fibroblasts during their transition from a migratory to a fibrogenic phenotype. Using atomic force microscopy we here show that part of this stronger adhesion is accomplished because OB-cadherin bonds resist ~twofold higher forces compared with N-cadherin junctions. By assessing the adhesion force between recombinant cadherin dimers and between native cadherins in the membrane of spread fibroblasts, we demonstrate that cadherin bonds are reinforced over time with two distinct force increments. By modulating the degree of lateral cadherin diffusion and F-actin organization we can attribute the resulting three force states to the single-molecule bond rather than to cadherin cluster formation. Notably, association with actin filaments enhances cadherin adhesion strength on the single-molecule level up to threefold; actin depolymerization reduces single-bond strength to the level of cadherin constructs missing the cytoplasmic domain. Hence, fibroblasts reinforce intercellular contacts by: (1) switching from N- to OB-cadherin expression; (2) increasing the strength of single-molecule bonds in three distinct steps; and (3) actin-promoted intrinsic activation of cadherin extracellular binding. We propose that this plasticity adapts fibroblast adhesions to the changing mechanical microenvironment of tissue under remodeling.

Supplementary material available online at
http://jcs.biologists.org/cgi/content/full/121/6/877/DC1

Key words: Atomic force microscopy, Myofibroblast, N-cadherin, OB-cadherin, Cytoskeleton

Introduction

Differentiation of fibroblasts into contractile myofibroblasts is a key event during the development of pathological contractures that characterize organ fibrosis and tissue reconstruction after wounding (Hinz, 2007). This transition occurs in two phases. The first phase involves the release of inflammatory cytokines and the altered mechanical properties of the extracellular matrix (ECM) following tissue injury initiate the formation of cytoplasmic actin stress fibers which hallmark the 'proto-myofibroblast' (Hinz and Gabbiani, 2003b); most fibroblastic cells acquire this phenotype in standard culture (Tomasek et al., 2002). The second phase occurs in the presence of pro-fibrotic cytokines, such as transforming growth factor β1 (TGFβ1) and mechanical stress, when proto-myofibroblasts further develop into 'differentiated myofibroblasts' by de novo expression of α-smooth muscle actin (α-SMA). Integration of α-SMA into stress fibers significantly augments myofibroblast contraction that is transmitted to the ECM at sites of specialized focal adhesions (Hinz et al., 2001; Hinz et al., 2003).

In addition, myofibroblasts couple stress fibers intercellularly via adherens junctions (AJs) (Hinz and Gabbiani, 2003a) by binding to the cytoplasmic domain of transmembrane cadherins through a catenin-containing complex (Gumbiner, 2005; Nagafuchi, 2001; Weis and Nelson, 2006; Wheelock and Johnson, 2003). Recently, we demonstrated that development of stress fibers in migratory proto-myofibroblasts of early wound tissue and in culture coincides with the initiation of N-cadherin (cadherin-2) containing AJs. In cells of mesenchymal origin including smooth muscle cells and fibroblasts (Hazan et al., 2000; Jones et al., 2002), during epithelial-to-mesenchymal transition (Thiery, 2002) and during transformation of epithelial cells in cancer (De Wever and Mareel, 2003), expression of N-cadherin is associated with acquisition of a migratory cell phenotype and rather transient contacts. By contrast, OB-cadherin expression in fibroblastic cells appears to be correlated with elevated levels of mechanical stress, such as in suburothelial myofibroblasts (Kuijpers et al., 2007) in pericryptal myofibroblasts (Cristia et al., 2005) and in differentiated myofibroblasts of contractile wounds (Hinz et al., 2004). Neo-expressed OB-cadherin (cadherin-11) gradually replaces N-cadherin in late contractile wounds and during TGFβ1-induced myofibroblast differentiation in culture. A similar switch to OB-cadherin expression is observed in stromal myofibroblasts surrounding epithelial tumors (Tomita et al., 2000). Inhibition of OB-cadherin, but not of N-cadherin, with specific peptides reduces the contraction of myofibroblast-populated collagen gels, indicating the importance of intercellular contacts in regulating ECM remodeling by myofibroblasts (Hinz et al., 2004). In a very recent work, we show that OB-cadherin-type AJs coordinate Ca^{2+} signaling and contraction between differentiated myofibroblasts; this is in contrast to N-cadherin, which plays no significant role in coordinating these activities between connected proto-myofibroblasts (L. Follonier, S. Schaub, J.-J.M. and B.H., unpublished results). Consistently, AJs of differentiated myofibroblasts exhibit higher mechanical resistance than AJs between proto-myofibroblasts as demonstrated by subjecting cell pairs to hydrodynamic force in a flow chamber. This stronger attachment is partly due to AJ reinforcement by α-SMA-generated high contractile activity; blocking this activity specifically reduces cell-cell adhesion (Hinz et al., 2004). It remains to be shown whether

in myofibroblasts OB-cadherin promotes stronger adhesion than N-cadherin on the single-bond level.

N- and OB-cadherin are classical cadherins characterized by five Ca^{2+}-dependent extracellular cadherin (EC) domains (Nollet et al., 2000; Patel et al., 2003; Troyanovsky, 2005; Williams et al., 2000). The number of EC domains contributing to trans-adhesion specificity and binding strength remains controversial (Chappuis-Flament et al., 2001; Troyanovsky, 2005; Zhu et al., 2003), although a primordial role of the EC1 domain is generally assumed (Harrison et al., 2005). Competitive inhibition of cell adhesion recognition sequences in the EC1 domain was shown to block cadherin-mediated adhesion (Blaschuk et al., 1990; Noe et al., 1999; Williams et al., 2000). Classical cadherins are further classified into type I and type II, according to the presence and absence of the His-Ala-Val (HAV) sequence in the EC1 domain (Blaschuk and Rowlands, 2002; Nollet et al., 2000); structural differences between the EC1 domains seem to prevent heterophilic interaction between the groups (Patel et al., 2006).

In the present study, we have evaluated whether the differential expression of N-cadherin (type I) in proto-myofibroblasts and of OB-cadherin (type II) in differentiated myofibroblasts contributes to the higher intercellular adhesion described for differentiated myofibroblasts. Using atomic force microscopy (AFM) we measured the interaction strength between N- and OB-cadherin dimer-coated surfaces (cadherin-cadherin set-up), between cadherin dimers and myofibroblasts grown in monolayers (cadherin-cell set-up) and between spread proto- and differentiated myofibroblasts (cell-cell set-up), respectively. In all experimental setups OB-cadherin junctions exhibited higher adhesion strength than N-cadherin junctions. Our data further support the idea that the forces measured with AFM resolution correspond to single-molecule cadherin dimer interactions, which can exhibit three distinct force states. In the cell-cell set-up, cytoplasmic interaction with the actin cytoskeleton further increases the intrinsic binding strength of OB-cadherin. We propose that mechanically stable OB-cadherin containing cell-cell contacts play an important role in coordinating the contraction of differentiated myofibroblasts to achieve efficient tissue remodeling.

Results

OB-cadherin junctions are stronger than N-cadherin bonds

Using western blotting and immunofluorescence, we have previously shown that the differentiation of contractile proto-myofibroblasts into highly contractile and strongly adherent differentiated myofibroblasts is correlated with a clear shift from N- to OB-cadherin expression (Hinz et al., 2004). To compare cadherin surface-expression levels in both cell types with flow cytometry, we analyzed rat subcutaneous fibroblasts attaining a proto-myofibroblast phenotype in control culture conditions and after treatment with TGFβ1, which generates differentiated myofibroblasts. Myofibroblast differentiation was assessed with antibodies against the differentiated myofibroblast marker α-SMA (supplementary material Fig. S1A). N-cadherin expression was significantly higher in α-SMA-negative proto-myofibroblasts than in α-SMA-positive differentiated myofibroblasts (supplementary material Fig. S1B). By contrast, expression of OB-cadherin was low in proto-myofibroblasts but high in differentiated myofibroblasts (supplementary material Fig. S1C). Thus, we worked with a physiologically relevant cell model in which a change in stress-fiber-connecting cadherins may be associated with the contractile function of the cell.

In a flow-chamber assay, differentiated myofibroblasts exhibit higher intercellular adhesion than proto-myofibroblasts (Hinz et al., 2004). Here, we wanted to elucidate whether this difference in

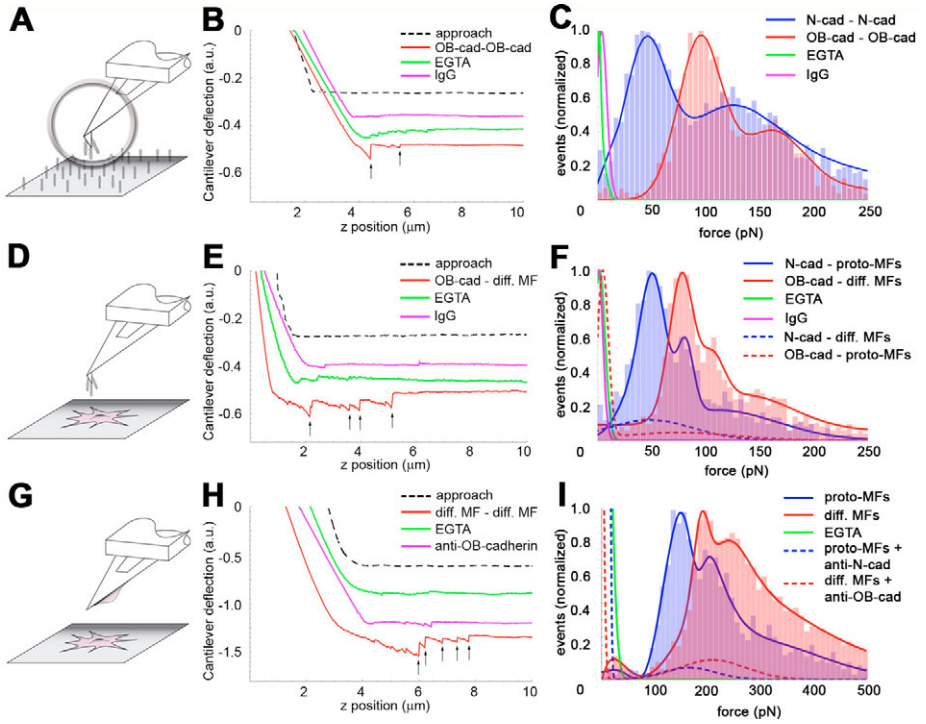

Fig. 1. Adhesion of differentiated myofibroblasts is stronger than that of proto-myofibroblasts. Adhesion forces are measured with AFM between cadherin dimer-coated cantilevers and similarly coated substrates (A-C), between cadherin dimer-coated cantilevers and myofibroblasts (D,E), and between myofibroblasts grown on cantilevers and myofibroblasts grown in monolayers (G-I). In all conditions, cantilever approach-retraction velocities were set to 0.1 μm/second, loading force to 3 nN and contact time to 2 seconds. (B,E,H) Typical force-distance curves under different conditions are displayed for each configuration; arrows indicate positions where bond rupture occurs in a 'jump'. Red profiles indicate typical interaction between OB- cadherins or differentiated myofibroblasts in the different set-ups, green lines represent controls in the absence of extracellular Ca^{2+} (EGTA) and pink lines show controls performed with IgG-coated cantilevers (B,E) or contacts formed in the presence of OB-cadherin-blocking peptides (H). (C,F,I) Rupture forces displayed as histograms ($n \geqslant 5000$ in each condition), normalized for the total number of rupture events in every configuration and fitted with Gaussian curves. Results obtained with proto-myofibroblasts and N-cadherin are displayed in blue, whereas results with differentiated myofibroblasts and OB-cadherin rupture forces are indicated in red. Note the different scale in H, which allows for the significantly higher bond strength in the cell-cell set-up compared with set-ups in B and E. Cadherin specificity of interactions was controlled by coating cantilevers with human IgG (C,F, pink), by using EGTA (green) and by applying anti-cadherin peptides (I, dashed lines).

overall adhesion relates to different adhesion strengths of N- and OB-cadherin on the single-molecule level. For this, we first coated AFM cantilever tips with N- or OB-cadherin:Fc dimers (10 μg/ml) that were put into contact with coated coverslips (Fig. 1A). Contact was established for 2 seconds with 0.1 μm/second approach velocity and 3 nN loading force and the bonds were then separated with the same retraction speed. Detachment events were determined from rapid changes in AFM cantilever deflection ('jumps') in force-distance curves (Fig. 1B arrows, supplementary material Fig. S2). The height of a jump was proportional to the force needed to separate one adhesive bond (supplementary material Fig. S2). For statistical evaluation, we assembled all measured forces in histograms and fitted the data with Gaussian curves. When putting recombinant cadherin-dimer-coated surfaces into contact, we obtained one major force peak for OB-cadherin (95±20 pN) (Fig. 1C, red) in Gaussian-fitted histograms of rupture forces, which was about twice the force obtained with N-cadherin (44±19 pN) (Fig. 2C, blue). A second peak appeared in histograms at 161±31 pN for OB-cadherin and at 120±44 pN for N-cadherin rupture forces (Fig. 1C). Controls with human IgG-coated cantilever tips excluded nonspecific interaction between the Fc domains of cadherin:Fc fusion proteins (Fig. 1B,C, green) and cadherin adhesion was abolished in the absence of Ca^{2+} (Fig. 1B,C, pink); heterotypic cadherin pairs did not interact. Hence, homotypic interaction between OB-cadherin bonds is stronger than that of N-cadherin, and both bond types formed with recombinant dimers exist in two principal force states after 2 seconds of contact.

To test the significance of N- and OB-cadherin adhesion in living myofibroblasts, we measured the interaction strength between cells grown on coverslips in monolayer and AFM cantilever tips coated with 10 μg/ml cadherin:Fc dimers (Fig. 1D). After 2 seconds of contact time using 0.1 μm/second approach-retraction velocities and 3 nN loading force, multiple rupture jumps preceded complete detachment (Fig. 1E, arrows). From the jump heights, we extracted that N-cadherin-coated cantilevers adhered to proto-myofibroblasts with a main average force of 54±9 pN, a secondary force of 79±8 pN and a third shoulder with a peak at 112±54 (Fig. 1F, blue) as seen in Gaussian-fitted histograms of all measured forces; virtually no interaction was observed between proto-myofibroblasts and OB-cadherin:Fc tips (Fig. 1F, dashed red fit). OB-cadherin:Fc adhered to differentiated myofibroblasts with higher forces of 80±12 pN (main peak), 108±21 pN (secondary peak) and 152±56 (third shoulder peak) (Fig. 1F, red). We occasionally observed adhesion between N-cadherin:Fc and differentiated myofibroblasts, occurring ~20 times less frequently, with a mean force of ~55 pN (Fig. 1F, dashed blue fit). IgG-coated cantilevers never promoted adhesion with cells (Fig. 1E,F, green) and EGTA completely inhibited cadherin-mediated interactions (Fig. 1E,F, pink). These results confirm that N-cadherin is the predominant cadherin in proto-myofibroblasts and that OB-cadherin is specific for differentiated myofibroblasts; the latter promoted higher adhesion.

Then, we assessed the strength of the respective cadherin bonds in their physiological context, i.e. including cis-interaction between monomers and/or dimers, their functional cytoplasmic tail and their cytosolic partners. For this we put myofibroblasts spread on tipless AFM cantilevers in contact with myofibroblasts grown in confluent monolayer (Fig. 1G). After 2 seconds of contact time using 0.1 μm/second approach-retraction velocities and 3 nN loading force, cells detached completely, undergoing multiple rupture events (Fig. 1H, arrows). Gaussian-fitted histograms of all rupture forces show that cadherins in myofibroblast plasma membranes adhered with three main forces: 141±21 pN, 200±48 pN and 274±130 pN in proto-myofibroblasts (Fig. 1I, blue) and 190±17 pN, 242±54 pN and 381±99 in differentiated myofibroblasts (Fig. 1I, red). No adhesion was measured in the absence of Ca^{2+} (Fig. 1H,I, EGTA, green). Rupture analysis in the cell-cell setup produced one additional low peak at ~100 pN, which may be due to membrane-related tethering effects because this population of rupture events is associated with particularly long movements of the AFM cantilever (data not shown). Considering each force peak separately, differentiated myofibroblasts always exhibited significantly stronger adhesion than proto-myofibroblasts. To corroborate the implication of N- and OB-cadherin in the cell-cell set-up, we added inhibitory peptides directed against the respective EC1 domain (Blaschuk et al., 1990; Hinz et al., 2004; Williams et al., 2000). Both anti-cadherin peptides significantly reduced the occurrence of rupture events (Fig. 1H, pink, supplementary material Fig. S3A-D). Anti-OB-cadherin reduced the frequency of binding events between differentiated myofibroblasts by ~85% (Fig. 1I, anti-OB-cad, red dashed line, supplementary material Fig. S3C); a similar reduction by ~90% was observed for proto-myofibroblasts in the presence of anti-N-

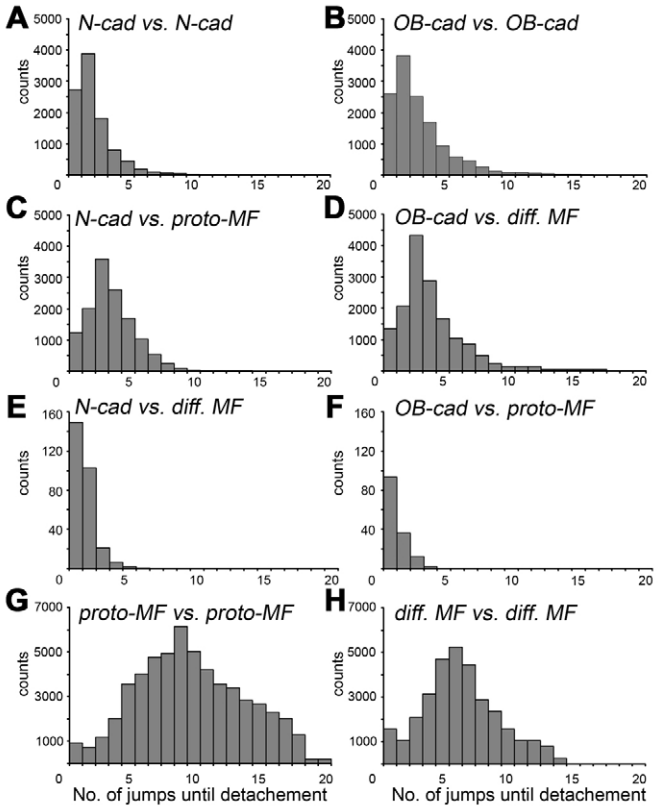

Fig. 2. De-adhesion of two cells occurs with multiple rupture events. Histograms summarize the number of rupture events (jumps) preceding the complete detachment of the cantilever from the touched (put into contact) respective substrate from all force-distance profiles (Fig. 1B,E,H). Different interaction setups were tested. Recombinant cadherin dimers grafted to AFM cantilevers were put into contact with carpets of the respective cadherin dimers (A,B) and with myofibroblasts grown in monolayer (C,D). Proto-myofibroblasts were put into contact with N-cadherin (C) and OB-cadherin (F) and differentiated myofibroblasts were put into contact with OB-cadherin (D) and N-cadherin (E). In the cell-cell setup, proto-myofibroblasts (G) and differentiated myofibroblasts (H) were spread on tipless AFM cantilevers and put into contact with the same cell type grown in monolayer. Cantilever approach-retraction velocities were set to 0.1 μm/second, loading force to 3 nN and contact time to 2 seconds.

cadherin (Fig. 1I, anti-N-cad, blue dashed line, supplementary material Fig. S3D). Adding anti-N-cadherin peptide to differentiated myofibroblasts (supplementary material Fig. S3A,E) and anti-OB-cadherin peptide to proto-myofibroblasts (supplementary material Fig. S3B,F) as well as control peptides (data not shown) was without effect. Together these results show that OB-cadherin bonds promote higher adhesion between differentiated myofibroblasts than N-cadherin bonds between proto-myofibroblasts. In all experimental set-ups with a 2 second contact time, we recorded a maximum of three force states for each cadherin type, of which the second and third were more pronounced when put into contact with native cadherins in living cells.

Differentiated myofibroblasts exhibit fewer but stronger intercellular bonds

In addition to the force of cadherin bonds (represented by the height of rupture jumps), the number of rupture events preceding separation of two surfaces contributes to overall adhesion strength. Quantifying the number of rupture jumps preceding total detachment in force-distance profiles after 2 seconds of contact (Fig. 1B,E,H arrows) demonstrated that the average number of rupture events preceding detachment of AFM cantilevers and surfaces coated with recombinant cadherins was 2.0±1.4 for both cadherin types (Fig. 1B, Fig. 2A,B). De-adhesion of N-cadherin-coated cantilevers from proto-myofibroblasts in monolayer occurred with an average of 3.7±1.4 rupture events (Fig. 1E, Fig. 2C), which was similar for separating recombinant OB-cadherin from differentiated myofibroblasts (Fig. 2D). The number of bonds formed and ruptured between N-cadherin and differentiated myofibroblasts as well as between OB-cadherin and proto-myofibroblasts was negligible (Fig. 2E,F). Complete separation of two cells occurred with a significantly higher number of jumps that differed between both cell types. On average, 8.9±4.3 rupture events preceded detachment of proto-myofibroblasts (Fig. 1H, Fig. 2G) and 5.9±2.4 rupture events occurred before differentiated myofibroblasts were separated (Fig. 2H). Hence, the higher total adhesion previously measured between differentiated myofibroblasts (Hinz et al., 2004) is achieved with a lower number of OB-cadherin bonds, which are however, stronger than the higher number of N-cadherin bonds in proto-myofibroblasts. At present, we cannot explain why the low levels of N-cadherin expressed on the surface of differentiated myofibroblasts as well as OB-cadherin on proto-myofibroblasts represent such a small fraction (~1%) of all bonds. It is conceivable that each cadherin type exhibits different activities depending on the cellular background of its expression.

OB-cadherin junctions exhibit three distinct force states

At this stage, the nature of the cadherin bond rupture jumps in the force-distance profiles are not defined. Two interpretations are possible: (1) each jump can correspond to the separation of one single-molecule cadherin bond which exists in three different force states after 2 seconds of contact time and (2) one jump can represent the simultaneous rupture of one to three cadherins that laterally (cis-) cooperate. To evaluate each possibility, we performed a series of additional experiments using recombinant OB-cadherin dimers and differentiated myofibroblasts. First, we analyzed only the heights of the last rupture events in cell-cell detachment profiles (supplementary material Fig. S2) and found three main force peaks in Gaussian-fitted histograms (Fig. 3A), which is comparable with the analysis of all rupture events (Fig. 3B). Occurrence of multiple force peaks in the last rupture analysis

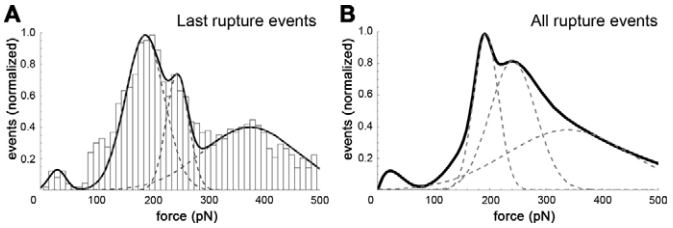

Fig. 3. Last rupture event analysis in force-distance profiles is similar to analysis of all rupture events. Differentiated myofibroblasts grown on tipless AFM cantilevers were connected with differentiated myofibroblasts grown in monolayer for 2 seconds with constant approach velocity (0.1 μm/second) and loading force (3 nN). (A) Results obtained by including only the last rupture events in force-distance profiles (supplementary material Fig. S2) are displayed as Gaussian curve fits of histograms, normalized to the total number of last rupture events (n>1000). Force distribution is comparable to the histogram obtained after analyzing all rupture jumps in force-distance profiles (n⩾5000) (Fig. 1I).

was unexpected if one jump comprises simultaneous rupture of multiple cadherin bonds, because only one single-molecule bond should remain under maximal tension after 'unzipping' two cell surfaces.

We tested whether interaction of the cytoplasmic portion of cell cadherins with the actin cytoskeleton augments the probability of multiple peaks in force histograms. The contractile actin cytoskeleton has been shown to increase intercellular adhesion by supporting lateral clustering of cadherins (Bershadsky, 2004; Chan et al., 2004; Chu et al., 2004; Delanoe-Ayari et al., 2004; El Sayegh et al., 2007; Gumbiner, 2000; Mege et al., 2006). To block this action, we put into contact differentiated myofibroblasts in the presence of cytochalasin D, which disassembled stress fibers of myofibroblasts on AFM cantilevers (Fig. 4A,B). Probing the topography of monolayer myofibroblasts with AFM in imaging mode (Fig. 4C) demonstrated cell surface smoothing as a result of disassembly of stress fibers and cell heightening due to cell relaxation (Fig. 4D). We then measured how cytochalasin D influences the strength of OB-cadherin bonds and displayed all rupture forces in Gaussian-fitted histograms (Fig. 4E). Compared with results obtained from two intact differentiated myofibroblasts that had been put into contact (Fig. 4E, black dashed line), actin depolymerization reduced the amplitude of the second force peak and reduced the third shoulder (Fig. 4E, black line). This result appears to suggest that the second and third force peaks are due to clustering of two and three cadherins, respectively. Most notably however, disrupting actin filaments also reduced the strength of native OB-cadherin bonds in the plasma membrane; this force-peak-position shift produced a force distribution profile very similar to that obtained from recombinant OB-cadherin dimers that had been put into contact (Fig. 4E, red line). Hence, it is possible that interaction of the cytoplasmic cadherin tail with actin filaments regulates the extracellular binding strength of single-molecule OB-cadherin, independently of clustering events.

Next, we increased the contact time between differentiated myofibroblasts, hypothesizing that longer contact times should increase the number of force peaks in histograms if force increase is due to cadherin clustering. Statistical analysis of force-distance curves in Gaussian histograms revealed that the average height of rupture jumps increased with longer contact times (Fig. 5A, supplementary material Fig. S4). Compared with 2 seconds of contact time (Fig. 5A, black, supplementary material Fig. S4),

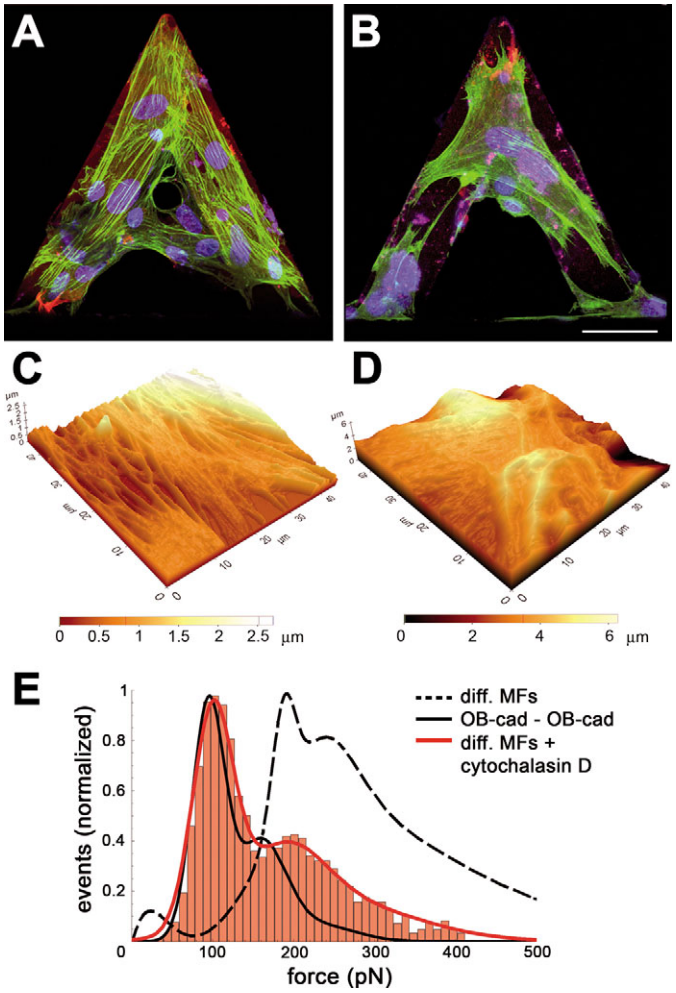

Fig. 4. Intracellular association with F-actin increases extracellular cadherin binding strength. (A,B) Differentiated myofibroblasts were grown on tipless AFM cantilevers in control conditions (A) or treated for 30 minutes with 1 µM cytochalasin D to depolymerize F-actin (B). Cells were immunostained for α-SMA (green) and nuclei (blue) and images were taken with a confocal microscope. (C,D) AFM was used in imaging mode to probe the topography of monolayer cells before (C) and after cytochalasin D treatment (D); false-color intensity increases with cell height. (E) Differentiated myofibroblasts grown on tipless AFM cantilevers were put into contact for 2 seconds with myofibroblasts grown in monolayer using 3 nN loading force and an approach velocity of 0.1 µm/second (n>1500). All measured rupture forces are accumulated in histograms that were fitted with Gaussian curves and normalized to the total number of events. Contact was performed in the presence of cytochalasin D (solid red line) and compared with histograms obtained by putting into contact differentiated myofibroblasts in control conditions (dashed black line) (Fig. 1I) and by putting into contact recombinant OB-cadherins (solid black line) (Fig. 1C). Note that actin depolymerization reduces intrinsic binding of native myofibroblast cadherins to the level of recombinant OB-cadherin dimers. Scale bar: 50 µm.

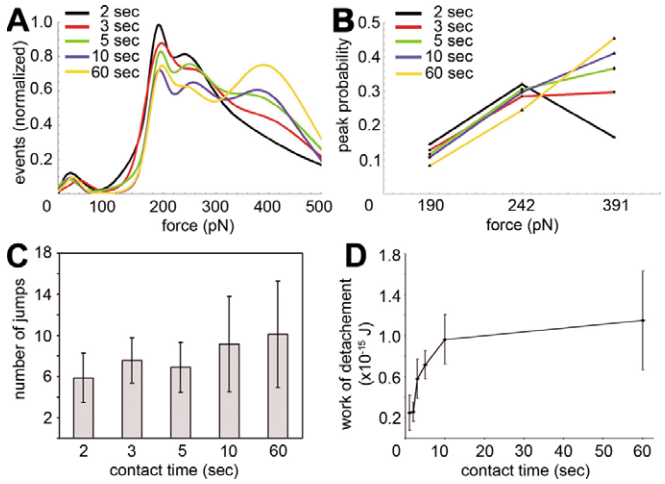

Fig. 5. The bond strength of native OB-cadherins in differentiated myofibroblasts increases with increasing contact time. Differentiated myofibroblasts grown on tipless AFM cantilevers were put into contact with differentiated myofibroblasts grown in monolayer using a constant approach velocity (0.1 µm/second) and loading force (3 nN). (A) All obtained rupture forces are displayed as histograms (n≥4000 per contact time), normalized for the total number of rupture events in every configuration and fitted with Gaussian curves. (B) With increasing contact time, the probability of obtaining three distinct force peaks increases; probability is calculated from the area under each individual Gaussian peak and divided by the total curve area (see supplementary material Fig. S2). (C) The average number of rupture jumps (±s.d.) preceding total cell detachment was determined in force-distance profiles for each contact time. (D) The total work needed to completely detach two differentiated myofibroblasts is displayed as a function of contact time (2-60 seconds).

contacts of 3 seconds augmented the occurrence of 242 pN (second peak) rupture events at the expense of decreased 190 pN adhesions (first peak) without altering the position of force peaks (Fig. 5A red, supplementary material Fig. S4). With contact times >3 seconds, the third peak at 381±78 pN became more prominent, further increasing after 10 seconds (Fig. 5C blue, supplementary material Fig. S4) and becoming most prominent after 60 seconds of contact (Fig. 5A orange, supplementary material Fig. S4). Notably, we never observed more than three significant force peaks, even after 60 seconds of contact time (Fig. 5A). By measuring the ratio of the areas under each Gaussian-fitted peak (supplementary material Fig. S4, dotted lines) and the total Gaussian curve area (supplementary material Fig. S4, solid lines), we obtained the statistical probability for the occurrence of each distinct force state at 190 pN, 242 pN and 381 pN (Fig. 5B). The probability for OB-cadherin junctions to obtain the higher force states increased with increasing contact time (Fig. 5B). When further analyzing the number of rupture events preceding complete cell separation we measured a moderate twofold increase from 5.9±2.4 after 2 seconds to 10.1±5.2 after 60 seconds of contact time (Fig. 5C). Finally, to investigate how contact time changes total cell-cell adhesion in the AFM setup, we determined the total work of (de-)adhesion from the surface included by the force-distance profile and the baseline; this reflects the total energy that needs to be invested to separate two myofibroblasts (supplementary material Fig. S2). Increasing contact times from 2 to 60 seconds significantly increased the work of total cell adhesion ~fivefold, reaching a maximum after 60 seconds (Fig. 5D). The fact that increasing contact time augments the force needed to induce single-bond ruptures, rather than increasing the number of engaged bonds, favors the existence of different force states of the single-molecule bond.

From the results above, it appears unlikely that multiple force peaks in Gaussian-fitted histograms correspond to simultaneously rupturing cadherin clusters. To finally eliminate cadherin diffusion and clustering, we put cantilever tips for 2-60 seconds into contact with glass surfaces, both provided with covalently bound recombinant OB-cadherin dimers (10 µg/ml) (Fig. 6). Comparable with the cell-cell experimental set-up (Fig. 5), we obtained a second

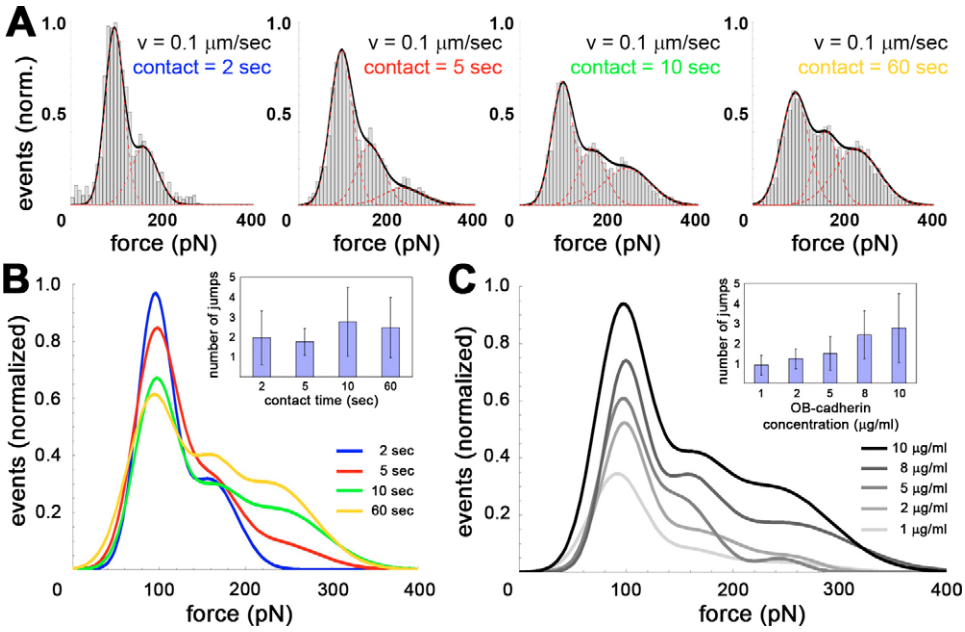

Fig. 6. The bond strength between recombinant cadherin dimers increases with increasing contact time. (A) AFM cantilevers coated with recombinant OB-cadherin (10 μg/ml) were put into contact with similarly coated surfaces, using a constant approach velocity (0.1 μm/second) and loading force (3 nN). All measured rupture forces are summarized in histograms that are fitted with Gaussian curves for contact times of 2, 5, 10 and 60 seconds ($n \geqslant 5000$ in each condition). Gaussian curves obtained after 5, 10, and 60 seconds contact time are normalized to the total number of events obtained after 2 seconds of contact time for direct comparison. The dashed lines represent Gaussian curve fits of single peaks that are included in each total data set. (B) Overlaying all Gaussian fits obtained for each contact time demonstrates increasing formation of a third force peak with increased contact time, at decreasing amplitude of the first peak. Inset in B shows the average number of rupture jumps (±s.d.) that precede complete separation of two recombinant OB-cadherin bonds after different contact times. (C) AFM cantilevers coated with 10 μg/ml recombinant OB-cadherin were put into contact with surfaces that exhibited recombinant OB-cadherin coatings in decreasing concentrations of 20, 10, 8, 5, 2, and 1 μg/ml ($n \geqslant 5000$ in each condition), using a constant approach velocity (0.1 μm/second), loading force (3 nN) and a contact time of 60 seconds. Inset in C shows the average number of rupture jumps (±s.d.) that precede complete separation of two recombinant OB-cadherin bonds as a function of cadherin density. Note that lowering cadherin concentration does not reduce the number of force peaks but rather decreases the average number of rupture events leading to complete bond separation.

and third force peak whose amplitudes increased with longer contact times (Fig. 6A,B). The number of rupture events leading to complete de-adhesion was largely independent of the contact time (Fig. 6B inset). We then put 10 μg/ml recombinant OB-cadherin-coated cantilevers into contact with surfaces coated with decreasing densities of recombinant OB-cadherin for 10 seconds: a condition where we have obtained three force peaks after 10 seconds of contact. Decreasing cadherin density, i.e. decreasing the probability of cadherin dimer oligomerization did not reduce the number of force peaks in Gaussian-fitted histograms (Fig. 6C). The amplitude reduction of the main peak indicates the decreasing probability of bond formation at low cadherin densities, i.e. the decreased number of total rupture events (Fig. 6C inset). Together, these data suggest that three distinct force peaks correspond to three discrete force states of the single-molecule cadherin dimer bond and not to simultaneous rupture of cadherin oligomers.

Higher force states of OB-cadherin junctions exhibit longer bond lifetimes

In addition to the force sustained by the single-molecule bond, its lifetime contributes to the stability of a junction. To evaluate the kinetics of OB-cadherin bond stability as a function of the force state, we estimated the equilibrium bond lifetime from the force shift in bond strength, occurring with increasing loading rate. This relation of bond lifetime and loading rate, or inversely of the unloading (separation) rate, is described by Bell's Model (Baumgartner et al., 2000; Bell, 1978; Evans and Ritchie, 1997; Panorchan et al., 2006a). By increasing the tip retraction velocity v_f from 0.1 to 1.0 μm/second at 2 seconds of contact time, we obtained force peak position shifts from 190 to 244 pN, from 242 to 313 pN and from 381 to 486 pN in Gaussian-fitted histograms of rupture forces (Fig. 7A). The obtained OB-cadherin bond rupture forces f_m, were then related to the loading rate r_f, defined as the product of the curve slope just before rupture and cantilever retraction velocity (supplementary material Fig. S2) (Panorchan et al., 2006a):

$$f_m = \frac{k_B T}{\chi_\beta} \ln\left(\frac{\chi_\beta r_f}{k_{off}^0 k_B T}\right). \quad (1)$$

The equilibrium dissociation rate (k_{off}^0), the bond lifetime ($1/k_{off}^0$) and its reactive compliance (χ_β) were determined by fitting rupture force as a function of loading rate r_f (k_B=Boltzmann's constant, T=absolute temperature) (Fig. 7C). The first OB-cadherin force peak yielded reactive compliance of 0.17 nm and bond lifetime of 3.1 seconds (k_{off}^0=0.32 second^{-1}); the second force state yielded reactive compliance of 0.13 nm and bond lifetime of 4.0 seconds (k_{off}^0=0.25 second^{-1}) and the third state exhibited a reactive compliance of 0.09 nm and a bond lifetime of 7.0 seconds (k_{off}^0=0.14 second^{-1}). These results are consistent with the fact that the formation probability of the strongest (third) force state is highest for contact times longer than 3 seconds (Fig. 5B).

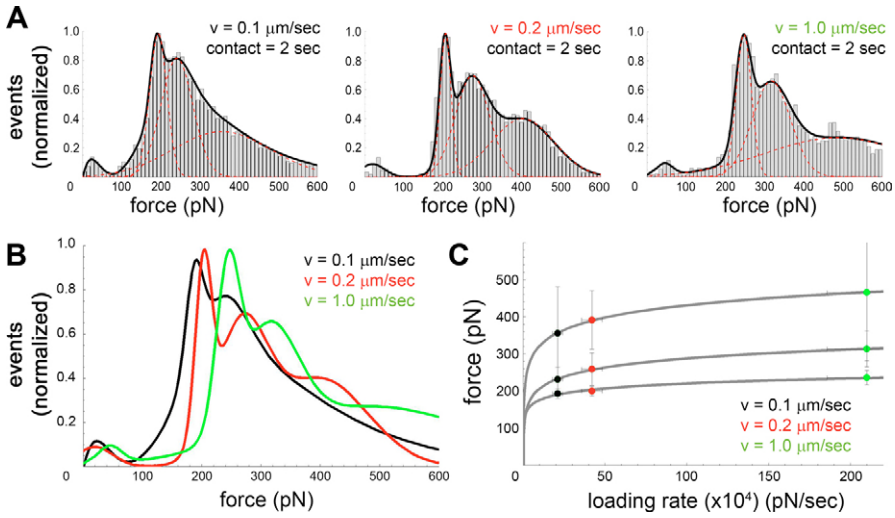

Fig. 7. Single-molecule bond strength of native cadherins in living myofibroblasts increases with increasing loading rate. (A) Differentiated myofibroblasts grown on tipless AFM cantilevers were put into contact for 2 seconds with myofibroblasts grown in a monolayer at 3 nN loading force and with approach velocities ranging from 0.1-1.0 μm/second (n>5000 per condition). All measured rupture forces are summarized in histograms that are fitted with Gaussian curves for approach velocities of 0.1, 0.2 and 1.0 μm/second, normalized to the total number of events. Dashed lines represent Gaussian fits of single peaks that are included in each total data set. (B) Overlaying all Gaussian fits obtained for each loading rate demonstrates a right shift in all Gaussian-fitted force peaks but no change in the number of peaks per histogram. (C) After fitting the data with Bell's model, force peak position is displayed as a function of the loading rate for each approach velocity.

Discussion

Cadherins promote specific cell recognition and sorting in a variety of different biological processes, tissues and cell types (Gumbiner, 2005; Hinz and Gabbiani, 2003a; Perez-Moreno et al., 2003; Shapiro et al., 2007; Tepass et al., 2000; Wheelock and Johnson, 2003). In addition, cadherins receive and transmit mechanical forces, which is evident from their association with the contractile actin cytoskeleton. Our data suggest that fibroblastic cells can increase intercellular adhesion by: (1) switching to a mechanically stronger cadherin type; (2) maturation of single-molecule cadherin bonds; (3) intrinsically increasing cadherin extracellular binding strength through cytoplasmic interaction with the actin filament system; and (4) cadherin clustering (which we do not assess in our study).

The physiological relevance of mechanically stronger AJs is suggestive considering the role of fibroblasts in the changing mechanical conditions during tissue repair and remodeling. The switch from N- to OB-cadherin expression is associated with the transition from low contractile and migratory proto-myofibroblasts, characterizing the proliferation phase of wound healing, to highly contractile differentiated myofibroblasts that promote wound contraction (Hinz et al., 2004). Forces of 10-50 nN are transmitted by N-cadherin-type junctions of cultured fibroblasts to deformable substrates (Ganz et al., 2006). To withstand the significantly higher stress generated by neo-incorporation of α-SMA into stress fibers (Hinz et al., 2001), AJs of cultured differentiated myofibroblasts increase in size; this maturation is blocked by inhibiting α-SMA contraction (Hinz et al., 2004). We have recently demonstrated that focal adhesions of differentiated myofibroblasts sustain ~fourfold higher stress of 12 nN/μm^2 compared with focal adhesions of α-SMA-negative proto-myofibroblasts (Goffin et al., 2006). Because the same stress is principally transmitted at sites of AJs it is conceivable that weaker N-cadherin bonds do not resist. Hence, the change in AJ molecular composition by de novo engagement of OB-cadherin appears to be analogous to the different integrin subsets and cytosolic proteins involved in myofibroblast focal adhesion maturation in response to enhanced mechanical challenge (Goffin et al., 2006).

Using AFM, we demonstrate that OB-cadherin bonds are always stronger than N-cadherin bonds; this is independent of whether we probed adhesion between cadherin dimers, between cadherin dimers and myofibroblasts, or between cadherins in the membrane of myofibroblasts. One possible explanation for this stronger adhesion is the structural difference between type II (OB-) and type I (N-) cadherins (Nollet et al., 2000; Patel et al., 2006). Other AFM studies demonstrated that type II VE-cadherin (cadherin-5) promotes stronger adhesion than type I N-cadherin; however, similar differences were reported in the same study between type I N- and E-cadherin (Panorchan et al., 2006b). No major differences were found between N- and VE-cadherin in another work using AFM and laser tweezers (Baumgartner et al., 2003), whereas dual-pipette assays revealed significantly stronger adhesion of cells expressing transfected type I E- and N-cadherin compared with type II cadherin-7 and OB-cadherin (Chu et al., 2006). One common finding of these studies is the absence of heterotypic interactions between type I and II cadherins (Patel et al., 2006). Hence, classification of cadherins into type I and II appears to play a role in homotypic recognition, but not in mediating a particular level of adhesion strength.

One important contribution of our study is the establishment of a physiologically relevant AFM setup to resolve single-molecule cadherin bond strength in the presence of the cytoplasmic tail, and the fact that we measure forces between native cadherins in their undisturbed (e.g. by cadherin overexpression) environment. Recombinant constructs lacking the cytoplasmic tail are widely used to measure interaction strengths of cadherins, that are grafted to AFM cantilevers, to microbeads in the biomembrane force probe (Baumgartner et al., 2000; du Roure et al., 2006; Perret et al., 2004), and hydrodynamic flow experiments (Pierres et al., 1998) or to the surface force apparatus (Leckband and Prakasam, 2006; Sivasankar et al., 1999). These methods assess function and attachment force of individual EC domains but cannot account for inside-out signaling (Bershadsky, 2004; Mege et al., 2006). On the other hand, estimating the force mediated by full-length cadherins between suspended cells in a dual-pipette assay (Chu et al., 2004) cannot resolve the single-bond strength. To measure the single-molecule interaction between native surface proteins of *Dictyostelium* (Benoit et al., 2000) and more recently of VE-, N- and E-cadherin, cells grown on AFM cantilevers put into contact with cells grown in a monolayer (Panorchan et al., 2006a; Panorchan et al., 2006b). In principle, this method allows the study of maturation of single-molecule bonds in the presence of inside-out regulation of cadherin activity, but this potential has not been explored because previous studies kept contact times extremely short (1 millisecond) (Panorchan et al., 2006b).

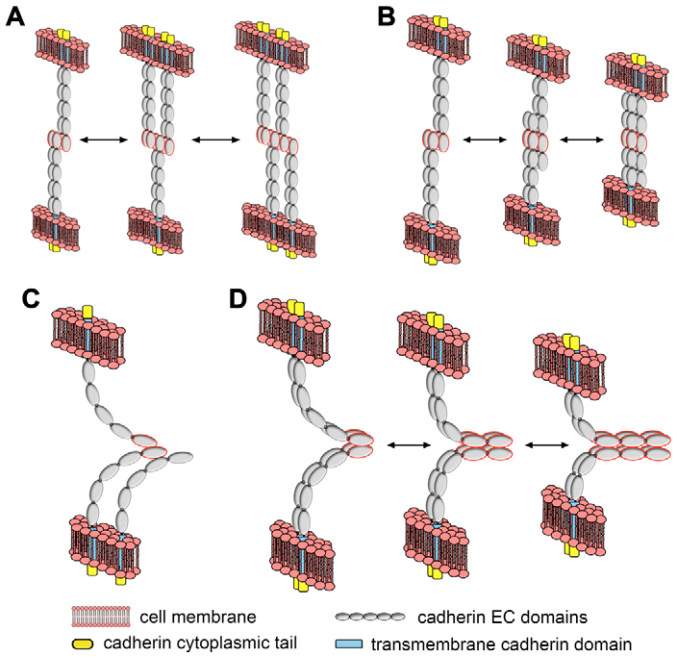

Fig. 8. Possible models for AJ reinforcement in differentiated myofibroblasts. In our experiments, the reinforcement of OB-cadherin bonds using either recombinant cadherin dimers or intact differentiated myofibroblasts, follows a sequence of maturation steps, always revealing three distinct force states. Different models can explain these states. (A) In the 'zipper' model, the EC1 domains of cadherin monomers or dimers (here presented for dimers) of two cells trans-interact. Multiple force states are created by increasing the number of laterally (cis-) associating cadherins in the plasma membrane. (B) The interdigitation model predicts that three force states are achieved at the single-molecule level. Here, consecutive and homotypic interdigitation of the EC domains 1-3 increases binding strength: being weak when EC1-EC1 interact, of medium strength during interaction of EC2-EC2 and strongest when the inner EC3-EC3 domains interact. (C) Models A and B are in conflict with structural data obtained from monomeric C-cadherin favoring a trans-'strand-dimer' model. Bent cadherin monomers trans-interact with their EC1 domains through binding of a flexible Trp residue to a hydrophobic pocket (not displayed). In addition to this trans-interaction, hydrophobic domains in EC1 and EC2 can cis-interact. To explain three distinct force states with this model, one has to assume multimer formation. (D) The synthesis of models B and C can explain both structural and functional data. Bent cadherins (here presented for dimers) trans-interact laterally through a sequence of homotypic EC domain interactions. With increasing alignment, this model predicts increasing single-bond strength and shortening of the junction. Owing to the rigid conformation of the cadherin molecules, more than three force states may be energetically unfavorable, but still possible. In all models, EC domains that contribute to trans binding are highlighted in red.

By using a similar cell-cell set-up with longer contact times we demonstrate that the weakest interaction forces between N- and OB-cadherins in the membrane of living cells (140-190 pN) are several times greater than those in recombinant cadherin dimers of the same type (44-80 pN) and as reported elsewhere for single E-cadherin fragments and recombinant VE-cadherin (20-75 pN) (Baumgartner et al., 2000; du Roure et al., 2006). Notably, actin depolymerization reduces the high adhesion between cell cadherins to the lower adhesion measured between recombinant cadherin dimers, indicating that interaction of the actin cytoskeleton with the cytoplasmic portion of cadherins intrinsically modulates their extracellular binding affinity. A number of studies have previously shown that reinforcement of cadherin junctions is mediated by the actin cytoskeleton (Bershadsky, 2004; Chan et al., 2004; Chu et al., 2004; Delanoe-Ayari et al., 2004; El Sayegh et al., 2007; Gumbiner, 2000; Mege et al., 2006; Shewan et al., 2005). Deletion of the cytoplasmic tail of E-cadherin, depolymerization of F-actin as well as interfering with actin polymerization by transfecting dominant-negative forms of Rac and Cdc42, all inhibit the maturation of E-cadherin junctions in cells suspended in a dual-pipette assay (Chu et al., 2004). However, it is important to note that these studies observed actin-mediated clustering of cadherins and reinforcement of AJ plaques over several minutes and using experimental set-ups that do not allow the measurement of forces at the single-bond level. By contrast, we here investigate and resolve the initial phase (2-60 seconds) of single cadherin-cadherin interaction that precedes clustering events (1-30 minutes). Thus, our results suggest that interaction of the cytoplasmic cadherin tail with F-actin has a direct effect on its extracellular binding activity. This may be analogous to the allosteric inside-out activation of integrins by unfolding the extracellular domains after interaction of the cytoplasmic part with the actin cytoskeleton (Cram and Schwarzbauer, 2004; Geiger et al., 2001; Ginsberg et al., 2005). A folded homo-associated form of E-cadherin has been consistently described in crystal structures (Pertz et al., 1999).

Although it is clear from our data that OB-cadherin bonds are stronger than N-cadherin bonds, the nature of these bonds, represented by one single rupture jump in AFM force-distance profiles, is less obvious. For both cadherin types, we resolved three predominant rupture jump heights in different experimental conditions. Three distinct rupture forces have previously been measured between recombinant VE-cadherin monomers in AFM experiments. Because the second and third force peaks were multiples of the first, the authors suggested simultaneous rupture of the respective number of cooperative monomers (Baumgartner et al., 2000) (Fig. 8A, here presented for dimers). Here, we observed three similar force states using cadherin dimers, which could be explained by zipping of cadherin dimers rather than monomer intercalation. However, neither 'zipper' models are supported by recent structural data, as discussed below (Koch et al., 2004; Shapiro et al., 2007; Troyanovsky, 2005). Moreover, several of our findings suggest that three force states may exist at the level of the single-molecule cadherin bond, rather than representing cadherin clustering. (1) Our results do not corroborate a quantum adhesion force and higher force peaks are no multiples of the first. (2) Even the highest rupture jumps that compose the third force peak occurred without any intermediate steps; that is, three single-molecule bonds should rupture simultaneously, which is unlikely to occur at the measured rate of events. (3) We never observed more than three statistically relevant force peaks even after increasing the contact time between two differentiated myofibroblasts up to 60 seconds. In this set-up, lateral diffusion of cadherin monomers and/or dimers is unlimited and the wide range of possible cis-interactions should produce multiple force peaks. (4) Minimizing the probability of cis-dimer cooperation by restricting the space for recombinant cadherins on the AFM cantilever tip and reducing cadherin concentration also produced three force states. (5) The three mean forces we obtained increased logarithmically with increasing loading rate; this shift in the force peak positions is consistent with Bell's model (Bell, 1978). Because of the stochastic nature of single-molecule bond formation, rupture forces follow a probability distribution that is defined by the energy landscape of the single bond and by the loading rate (Bayas et al., 2006; du Roure et al., 2006; Panorchan et al., 2006b). Our calculations imply a lifetime of ~3-4 seconds for the two lower

force states and more than 7 seconds for the third and strongest force state of OB-cadherin bonds. This is higher, but in the same order of magnitude, of single-bond lifetimes measured for VE-cadherin (2.2 seconds), N-cadherin (0.98 seconds) and E-cadherin (0.92 seconds) in a cell-cell set-up (Panorchan et al., 2006a).

One possible model to explain the three force states at the single-molecule bond level proposes homotypic EC domain interdigitation of cadherin dimers, based on distance measurements between cadherin-coated surfaces (Bayas et al., 2006; Chappuis-Flament et al., 2001; Leckband and Prakasam, 2006; Zhu et al., 2003). This model suggests a hierarchy of strengths, with the outer EC1-EC1 bond being the weakest, followed by medium EC2-EC2 adhesion and the strongest interaction between the inner EC3-EC3 pairs (Fig. 8B). However, this view of interdigitating EC domains between cadherin dimers appears to contradict structural data obtained with the entire extracellular region of the type I C-cadherin monomer (Boggon et al., 2002), which supports the 'strand-dimer' model (Fig. 8C). Several studies suggest that during trans interactions of type I cadherin monomers, a flexible Trp2 residue of one EC1 domain inserts into a hydrophobic pocket in the opposing EC1 domain and vice versa (Boggon et al., 2002; Parisini et al., 2007; Patel et al., 2003; Shapiro et al., 2007); a comparable but distinct mechanism has been proposed for type II cadherins (Patel et al., 2006). Structural data further suggest a lateral (cis-) exchange between hydrophobic residues in EC1 and EC2; this interaction includes the linker region between EC2 and EC3 (Boggon et al., 2002; Parisini et al., 2007) (Fig. 8C). It remains elusive how the strand-dimer model can explain the three force states obtained in our experiments, and that of others, with recombinant dimers – a conformation that does not exist in this model but that has been shown to be important for cadherin function (Chen et al., 2005). Very recently, force data obtained with the highly sensitive 'intermolecular force microscopy', revealed three to four force peaks for the single-molecule interaction between E-cadherin:Fc chimeras (Tsukasaki et al., 2007). The authors present an alternative model that may be congruent with both the 'strand-dimer' model and the EC interdigitation model (Fig. 8D). A future challenge will be to match structural information with functional data obtained with native cadherins in a physiological cell environment.

Materials and Methods

Cell culture and drugs

Primary rat subcutaneous fibroblasts expressing low levels of α-SMA (proto-myofibroblasts) were differentiated into α-SMA-positive myofibroblasts by adding TGFβ1 for 5 days to the culture medium (5 ng/ml, R&D Systems, Minneapolis, MN) (Hinz et al., 2004). Cell-surface proteins were preserved by trypsinization in the presence of 2 mM Ca^{2+} and by using DMEM, 10% FCS, 20 mM HEPES experimental medium, containing a final concentration of 2 mM Ca^{2+}. Controls demonstrating Ca^{2+} specificity of interactions were performed without Ca^{2+} and with 2 mM EGTA. Actin was depolymerized with 1 μM Cytochalasin D (Sigma Chemical, Buchs, Switzerland). Inhibitory peptides directed against OB- and N-cadherin (Adherex Technologies, Research Triangle Park, Durham, NC) were used at 1 mg/ml; sequence-scrambled peptides served as controls (Hinz et al., 2004).

AFM force measurements

Adhesion strength between single-molecule cadherins was evaluated by force-distance measurements using AFM (Cappella and Dietler, 1999) equipped with a liquid cell (XE-120, PSIA, Suwon, South Korea) and a self-developed program to control cantilever approach and retraction velocities (0.1-1.0 μm/second), contact time (1-60 seconds) and loading force (3 nN). Selected experiments were performed with a life science AFM (NanoWizard II, JPK, Berlin). Jumps in the cantilever deflection signal graph corresponded to the rupture of cadherin bonds (supplementary material Fig. S2). The height of all jumps was analyzed using self-developed software to calculate the corresponding adhesion force (pN) by considering the cantilever spring constant (pN/nm). Adhesion forces of all rupture events ($n \geq 4500$ per condition) were collected in histograms fitted with Gaussian curves (Baumgartner et al., 2000). In addition, we measured the work of total cell detachment (pN μm) from the area above retraction curves (supplementary material Fig. S2).

To assess the strength of native cadherins in living cells, we micromanipulated single myofibroblast onto tipless triangular silicon nitride cantilevers (200×50 μm, spring constant: 0.12±0.03 N/m, Veeco Instruments SAS, Dourdan, France). To promote cell spreading for 1-3 days, the cantilever was silanized with 2% (3-aminopropyl)triethoxy-silane (Sigma Chemical, Buchs, Switzerland), functionalized with 0.2% glutaraldehyde and coated with a 10 μg/ml fibronectin (Invitrogen AG, Basel, Switzerland). To measure recombinant cadherin adhesion, pyramidal tip triangular cantilevers (spring constant: 0.01±0.004 N/m, Veeco Instruments SAS) were equally functionalized and coated with 10 μg/ml Fc-fusion protein of N- or OB-cadherin dimers (R&D Systems). Insertion of a flexible linker between cadherins and the functionalized surface does not alter cadherin interaction force (du Roure et al., 2006), as confirmed with our experiments. As a control coating, we used human IgG (Sigma) at 10 μg/ml. Cell-, cadherin:Fc- and IgG-coated cantilevers were put into contact with a confluent monolayer of cells, grown for 5 days on glass coverslips and with similarly cadherin-coated surfaces.

Immunofluorescence and flow cytometry

Cells were fixed with 3% paraformaldehyde in PBS, permeabilized with 0.2% Triton X-100 in PBS and stained for α-SMA (anti-αSM-1) (Skalli et al., 1986), followed by Alexa Fluor 568 secondary anti-mouse antibodies (Molecular Probes, Eugene, OR). Cell nuclei were stained with DAPI (Sigma). Images were acquired with a 40× 1.25 NA objective on a confocal microscope (DM RXA2 with TCS SP2 AOBS, Leica, Glattbrugg, Switzerland). For FACS (FACScan, CyanADP, DAKO, Glostrup, Denmark), cells were trypsinized in the presence of 2 mM Ca^{2+}, processed as above and stained against N-cadherin (mIgG1, Transduction Laboratories Lexington, KY; rb, Santa Cruz, Heidelberg, Germany), OB-cadherin [mIgG1, J. A. Schalken, University Hospital Nijmegen, The Netherlands (Tomita et al., 2000); rb, R. M. Mège, INSERM U440, Paris, France (Marthiens et al., 2002)] and α-SMA (mIgG2a). As secondary antibodies, we used anti-mIgG2a-Alexa Fluor 647, anti-rb-Alexa Fluor 405 (Molecular Probes) and anti-mIgG1 (Southern Biotechnology Associates, Birmingham, AL).

J. Smith-Clerc and J. Roberts are acknowledged for technical assistance and C. Guzman for expert training and technical advice. We thank M. Lekka for carefully reading the manuscript and are grateful to Adherex Technologies Inc. (Research Triangle Park, Durham, NC) for providing anti-cadherin peptides. This work was supported by grants from the Swiss National Science Foundation (#3100A0-102150/1 and #3100A0-113733/1), from the Service Académique, EPFL and from the Competence Centre for Materials Science and Technology (CCMX) of the ETH-Board, Switzerland to B.H.

References

Baumgartner, W., Hinterdorfer, P., Ness, W., Raab, A., Vestweber, D., Schindler, H. and Drenckhahn, D. (2000). Cadherin interaction probed by atomic force microscopy. *Proc. Natl. Acad. Sci. USA* **97**, 4005-4010.

Baumgartner, W., Golenhofen, N., Grundhofer, N., Wiegand, J. and Drenckhahn, D. (2003). Ca^{2+} dependency of N-cadherin function probed by laser tweezer and atomic force microscopy. *J. Neurosci.* **23**, 11008-11014.

Bayas, M. V., Leung, A., Evans, E. and Leckband, D. (2006). Lifetime measurements reveal kinetic differences between homophilic cadherin bonds. *Biophys. J.* **90**, 1385-1395.

Bell, G. I. (1978). Models for the specific adhesion of cells to cells. *Science* **200**, 618-627.

Benoit, M., Gabriel, D., Gerisch, G. and Gaub, H. E. (2000). Discrete interactions in cell adhesion measured by single-molecule force spectroscopy. *Nat. Cell Biol.* **2**, 313-317.

Bershadsky, A. (2004). Magic touch: how does cell-cell adhesion trigger actin assembly? *Trends Cell Biol.* **14**, 589-593.

Blaschuk, O. W. and Rowlands, T. M. (2002). Plasma membrane components of adherens junctions (Review). *Mol. Membr. Biol.* **19**, 75-80.

Blaschuk, O. W., Sullivan, R., David, S. and Pouliot, Y. (1990). Identification of a cadherin cell adhesion recognition sequence. *Dev. Biol.* **139**, 227-229.

Boggon, T. J., Murray, J., Chappuis-Flament, S., Wong, E., Gumbiner, B. M. and Shapiro, L. (2002). C-cadherin ectodomain structure and implications for cell adhesion mechanisms. *Science* **296**, 1308-1313.

Cappella, B. and Dietler, G. (1999). Force-distance curves by atomic force microscopy. *Surf. Sci. Rep.* **34**, 1-104.

Chan, M. W., El Sayegh, T. Y., Arora, P. D., Laschinger, C. A., Overall, C. M., Morrison, C. and McCulloch, C. A. (2004). Regulation of intercellular adhesion strength in fibroblasts. *J. Biol. Chem.* **279**, 41047-41057.

Chappuis-Flament, S., Wong, E., Hicks, L. D., Kay, C. M. and Gumbiner, B. M. (2001). Multiple cadherin extracellular repeats mediate homophilic binding and adhesion. *J. Cell Biol.* **154**, 231-243.

Chen, C. P., Posy, S., Ben-Shaul, A., Shapiro, L. and Honig, B. H. (2005). Specificity of cell-cell adhesion by classical cadherins: critical role for low-affinity dimerization through beta-strand swapping. *Proc. Natl. Acad. Sci. USA* **102**, 8531-8536.

Chu, Y. S., Thomas, W. A., Eder, O., Pincet, F., Perez, E., Thiery, J. P. and Dufour, S. (2004). Force measurements in E-cadherin-mediated cell doublets reveal rapid adhesion strengthened by actin cytoskeleton remodeling through Rac and Cdc42. *J. Cell Biol.* **167**, 1183-1194.

Chu, Y. S., Eder, O., Thomas, W. A., Simcha, I., Pincet, F., Ben-Ze'ev, A., Perez, E., Thiery, J. P. and Dufour, S. (2006). Prototypical type I E-cadherin and type II cadherin-7 mediate very distinct adhesiveness through their extracellular domains. *J. Biol. Chem.* **281**, 2901-2910.

Cram, E. J. and Schwarzbauer, J. E. (2004). The talin wags the dog: new insights into integrin activation. *Trends Cell Biol.* **14**, 55-57.

Cristia, E., Afzal-Ahmed, I., Perez-Bosque, A., Amat, C., Naftalin, R. J. and Moreto, M. (2005). Pericryptal myofibroblast growth in rat descending colon induced by low-sodium diets is mediated by aldosterone and not by angiotensin II. *J. Membr. Biol.* **206**, 53-59.

Delanoe-Ayari, H., Al Kurdi, R., Vallade, M., Gulino-Debrac, D. and Riveline, D. (2004). Membrane and acto-myosin tension promote clustering of adhesion proteins. *Proc. Natl. Acad. Sci. USA* **101**, 2229-2234.

De Wever, O. and Mareel, M. (2003). Role of tissue stroma in cancer cell invasion. *J. Pathol.* **200**, 429-447.

du Roure, O., Buguin, A., Feracci, H. and Silberzan, P. (2006). Homophilic interactions between cadherin fragments at the single molecule level: an AFM study. *Langmuir* **22**, 4680-4684.

El Sayegh, T. Y., Kapus, A. and McCulloch, C. A. (2007). Beyond the epithelium: cadherin function in fibrous connective tissues. *FEBS Lett.* **581**, 167-174.

Evans, E. and Ritchie, K. (1997). Dynamic strength of molecular adhesion bonds. *Biophys. J.* **72**, 1541-1555.

Ganz, A., Lambert, M., Saez, A., Silberzan, P., Buguin, A., Mege, R. M. and Ladoux, B. (2006). Traction forces exerted through N-cadherin contacts. *Biol. Cell* **98**, 721-730.

Geiger, B., Bershadsky, A., Pankov, R. and Yamada, K. M. (2001). Transmembrane crosstalk between the extracellular matrix-cytoskeleton crosstalk. *Nat. Rev. Mol. Cell Biol.* **2**, 793-805.

Ginsberg, M. H., Partridge, A. and Shattil, S. J. (2005). Integrin regulation. *Curr. Opin. Cell Biol.* **17**, 509-516.

Goffin, J. M., Pittet, P., Csucs, G., Lussi, J. W., Meister, J. J. and Hinz, B. (2006). Focal adhesion size controls tension-dependent recruitment of alpha-smooth muscle actin to stress fibers. *J. Cell Biol.* **172**, 259-268.

Gumbiner, B. M. (2000). Regulation of cadherin adhesive activity. *J. Cell Biol.* **148**, 399-404.

Gumbiner, B. M. (2005). Regulation of cadherin-mediated adhesion in morphogenesis. *Nat. Rev. Mol. Cell Biol.* **6**, 622-634.

Harrison, O. J., Corps, E. M., Berge, T. and Kilshaw, P. J. (2005). The mechanism of cell adhesion by classical cadherins: the role of domain 1. *J. Cell Sci.* **118**, 711-721.

Hazan, R. B., Phillips, G. R., Qiao, R. F., Norton, L. and Aaronson, S. A. (2000). Exogenous expression of N-cadherin in breast cancer cells induces cell migration, invasion, and metastasis. *J. Cell Biol.* **148**, 779-790.

Hinz, B. (2007). Formation and function of the myofibroblast during tissue repair. *J. Invest. Dermatol.* **127**, 526-537.

Hinz, B. and Gabbiani, G. (2003a). Cell-matrix and cell-cell contacts of myofibroblasts: role in connective tissue remodeling. *Thromb. Haemost.* **90**, 993-1002.

Hinz, B. and Gabbiani, G. (2003b). Mechanisms of force generation and transmission by myofibroblasts. *Curr. Opin. Biotechnol.* **14**, 538-546.

Hinz, B., Celetta, G., Tomasek, J. J., Gabbiani, G. and Chaponnier, C. (2001). Alpha-smooth muscle actin expression upregulates fibroblast contractile activity. *Mol. Biol. Cell* **12**, 2730-2741.

Hinz, B., Dugina, V., Ballestrem, C., Wehrle-Haller, B. and Chaponnier, C. (2003). Alpha-smooth muscle actin is crucial for focal adhesion maturation in myofibroblasts. *Mol. Biol. Cell* **14**, 2508-2519.

Hinz, B., Pittet, P., Smith-Clerc, J., Chaponnier, C. and Meister, J. J. (2004). Myofibroblast development is characterized by specific cell-cell adherens junctions. *Mol. Biol. Cell* **15**, 4310-4320.

Jones, M., Sabatini, P. J., Lee, F. S., Bendeck, M. P. and Langille, B. L. (2002). N-cadherin upregulation and function in response of smooth muscle cells to arterial injury. *Arterioscler. Thromb. Vasc. Biol.* **22**, 1972-1977.

Koch, A. W., Manzur, K. L. and Shan, W. (2004). Structure-based models of cadherin-mediated cell adhesion: the evolution continues. *Cell. Mol. Life Sci.* **61**, 1884-1895.

Kuijpers, K. A., Heesakkers, J. P., Jansen, C. F. and Schalken, J. A. (2007). Cadherin-11 is expressed in detrusor smooth muscle cells and myofibroblasts of normal human bladder. *Eur. Urol.* **52**, 1213-1221.

Leckband, D. and Prakasam, A. (2006). Mechanism and dynamics of cadherin adhesion. *Annu. Rev. Biomed. Eng.* **8**, 259-2287.

Marthiens, V., Padilla, F., Lambert, M. and Mege, R. M. (2002). Complementary expression and regulation of cadherins 6 and 11 during specific steps of motoneuron differentiation. *Mol. Cell. Neurosci.* **20**, 458-475.

Mege, R. M., Gavard, J. and Lambert, M. (2006). Regulation of cell-cell junctions by the cytoskeleton. *Curr. Opin. Cell Biol.* **18**, 541-548.

Nagafuchi, A. (2001). Molecular architecture of adherens junctions. *Curr. Opin. Cell Biol.* **13**, 600-603.

Noe, V., Willems, J., Vandekerckhove, J., Roy, F. V., Bruyneel, E. and Mareel, M. (1999). Inhibition of adhesion and induction of epithelial cell invasion by HAV-containing E-cadherin-specific peptides. *J. Cell Sci.* **112**, 127-135.

Nollet, F., Kools, P. and van Roy, F. (2000). Phylogenetic analysis of the cadherin superfamily allows identification of six major subfamilies besides several solitary members. *J. Mol. Biol.* **299**, 551-572.

Panorchan, P., George, J. P. and Wirtz, D. (2006a). Probing intercellular interactions between vascular endothelial cadherin pairs at single-molecule resolution and in living cells. *J. Mol. Biol.* **358**, 665-674.

Panorchan, P., Thompson, M. S., Davis, K. J., Tseng, Y., Konstantopoulos, K. and Wirtz, D. (2006b). Single-molecule analysis of cadherin-mediated cell-cell adhesion. *J. Cell Sci.* **119**, 66-74.

Parisini, E., Higgins, J. M., Liu, J. H., Brenner, M. B. and Wang, J. H. (2007). The crystal structure of human E-cadherin domains 1 and 2, and comparison with other cadherins in the context of adhesion mechanism. *J. Mol. Biol.* **373**, 401-411.

Patel, S. D., Chen, C. P., Bahna, F., Honig, B. and Shapiro, L. (2003). Cadherin-mediated cell-cell adhesion: sticking together as a family. *Curr. Opin. Struct. Biol.* **13**, 690-698.

Patel, S. D., Ciatto, C., Chen, C. P., Bahna, F., Rajebhosale, M., Arkus, N., Schieren, I., Jessell, T. M., Honig, B., Price, S. R. et al. (2006). Type II cadherin ectodomain structures: implications for classical cadherin specificity. *Cell* **124**, 1255-1268.

Perez-Moreno, M., Jamora, C. and Fuchs, E. (2003). Sticky business: orchestrating cellular signals at adherens junctions. *Cell* **112**, 535-548.

Perret, E., Leung, A., Feracci, H. and Evans, E. (2004). Trans-bonded pairs of E-cadherin exhibit a remarkable hierarchy of mechanical strengths. *Proc. Natl. Acad. Sci. USA* **101**, 16472-16477.

Pertz, O., Bozic, D., Koch, A. W., Fauser, C., Brancaccio, A. and Engel, J. (1999). A new crystal structure, Ca^{2+} dependence and mutational analysis reveal molecular details of E-cadherin homoassociation. *EMBO J.* **18**, 1738-1747.

Pierres, A., Feracci, H., Delmas, V., Benoliel, A. M., Thiery, J. P. and Bongrand, P. (1998). Experimental study of the interaction range and association rate of surface-attached cadherin 11. *Proc. Natl. Acad. Sci. USA* **95**, 9256-9261.

Shapiro, L., Love, J. and Colman, D. R. (2007). Adhesion molecules in the nervous system: structural insights into function and diversity. *Annu. Rev. Neurosci.* **30**, 451-474.

Shewan, A. M., Maddugoda, M., Kraemer, A., Stehbens, S. J., Verma, S., Kovacs, E. M. and Yap, A. S. (2005). Myosin 2 is a key Rho kinase target necessary for the local concentration of E-cadherin at cell-cell contacts. *Mol. Biol. Cell* **16**, 4531-4542.

Sivasankar, S., Brieher, W., Lavrik, N., Gumbiner, B. and Leckband, D. (1999). Direct molecular force measurements of multiple adhesive interactions between cadherin ectodomains. *Proc. Natl. Acad. Sci. USA* **96**, 11820-1184.

Skalli, O., Ropraz, P., Trzeciak, A., Benzonana, G., Gillessen, D. and Gabbiani, G. (1986). A monoclonal antibody against alpha-smooth muscle actin: a new probe for smooth muscle differentiation. *J. Cell Biol.* **103**, 2787-2796.

Tepass, U., Truong, K., Godt, D., Ikura, M. and Peifer, M. (2000). Cadherins in embryonic and neural morphogenesis. *Nat. Rev. Mol. Cell Biol.* **1**, 91-100.

Thiery, J. P. (2002). Epithelial-mesenchymal transitions in tumour progression. *Nat. Rev. Cancer* **2**, 442-454.

Tomasek, J. J., Gabbiani, G., Hinz, B., Chaponnier, C. and Brown, R. A. (2002). Myofibroblasts and mechano-regulation of connective tissue remodelling. *Nat. Rev. Mol. Cell Biol.* **3**, 349-363.

Tomita, K., van Bokhoven, A., van Leenders, G. J., Ruijter, E. T., Jansen, C. F., Bussemakers, M. J. and Schalken, J. A. (2000). Cadherin switching in human prostate cancer progression. *Cancer Res.* **60**, 3650-3654.

Troyanovsky, S. (2005). Cadherin dimers in cell-cell adhesion. *Eur. J. Cell Biol.* **84**, 225-233.

Tsukasaki, Y., Kitamura, K., Shimizu, K., Iwane, A. H., Takai, Y. and Yanagida, T. (2007). Role of multiple bonds between the single cell adhesion molecules, nectin and cadherin, revealed by high sensitive force measurements. *J. Mol. Biol.* **367**, 996-1006.

Weis, W. I. and Nelson, W. J. (2006). Re-solving the cadherin-catenin-actin conundrum. *J. Biol. Chem.* **281**, 35593-35597.

Wheelock, M. J. and Johnson, K. R. (2003). Cadherins as modulators of cellular phenotype. *Annu. Rev. Cell Dev. Biol.* **19**, 207-235.

Williams, E. J., Williams, G., Gour, B., Blaschuk, O. and Doherty, P. (2000). INP, a novel N-cadherin antagonist targeted to the amino acids that flank the HAV motif. *Mol. Cell. Neurosci.* **15**, 456-464.

Zhu, B., Chappuis-Flament, S., Wong, E., Jensen, I. E., Gumbiner, B. M. and Leckband, D. (2003). Functional analysis of the structural basis of homophilic cadherin adhesion. *Biophys. J.* **84**, 4033-4042.